Styrene–Butadiene Rubber Membranes for the Pervaporative Separation of Benzene/Cyclohexane Mixtures

Hassiba Benguergoura, Saad Moulay

Laboratoire de Chimie-Physique Moléculaire et Macromoléculaire, Département de Chimie Industrielle, Faculté des Sciences de L'Ingénieur, Département de Chimie, Faculté des Sciences, Université Saad Dahlab de Blida, Blida, Algeria

Received 5 February 2010; accepted 19 December 2010
DOI 10.1002/app.34105
Published online 16 August 2011 in Wiley Online Library (wileyonlinelibrary.com).

ABSTRACT: Styrene–butadiene rubber membranes with methylene bridges, stemming from the concomitant *in situ* Friedel–Crafts alkylation during a chloromethylation reaction, were prepared and used in the pervaporative separation of benzene/cyclohexane mixtures. A set of four membranes with different crosslinking extents was achieved by the variation of the [Trimethylchlorosilane (TMCS)]/[Paraformaldehyde (PF)] molar ratios with respect to the styrene (St) unit. Study of the swelling of membranes by the mixture components individually and by their feed mixture compositions, 1 : 1 and 1 : 9, was conducted. The total flux (J) and the separation factor (α) were assessed as a function of the feed composition, temperature, and [St unit]/[TMCS]/[PF] molar ratios. The highest J and α measured in this study were 1401 g m^{-2} h^{-1} and 28.50, respectively. The diffusion selectivity was found to depend on the crosslinking extent of the membrane. © 2011 Wiley Periodicals, Inc. J Appl Polym Sci 123: 1455–1467, 2012

Key words: crosslinking; membranes; rubber; separation techniques; swelling

INTRODUCTION

The separation of liquid organics having close boiling points, or being azeotropic mixtures, isomers, or heat-sensitive mixtures, is better performed by the pervaporation technique, mainly because of its simplicity and cost effectiveness. Not only has pervaporation been a convenient process for the separation of mixtures, but its performance also has been extended to other undertakings such as the control of organic reactions[1–5] and the breakdown of microemulsions.[6–8] That pervaporation has gained a weighty foothold in separation processes on a laboratory scale is owed to the diversity of membrane types, which, in turn, is due to the availability of polymeric materials.[9] A membrane is selected for the separation of binary mixtures according to its solubility parameter (δ_m) vis-à-vis that of one of the two components (δ_i); that is, the closer δ_m is to δ_i, the more selective the membrane will be for component i, and the better the separation will be.[10] Other criteria with respect to the membrane should also be taken into account: (1) membranes should not swell substantially as the selectivity decreases drastically, (2) low swelling will result in low flux, and (3) crosslinking may reduce the excessive swelling, but it will negatively affect the permeation rate.

In the membrane-separative processes, the chemical nature of the membrane, among other aforementioned considerations, greatly affects the separation performance. According to the extent of organophilicity (or hydrophilicity), the membrane is selected for a particular application. Thus, the choice of a membrane has been always a central preoccupation when separation is intended. In this preoccupation, that is, the separation of a benzene (Bz)–cyclohexane (Cx) mixture by pervaporation, we were interested in styrene–butadiene rubber (SBR) material as a membrane for such a goal.

Membranes made exclusively with polystyrene (PS), a plastic material, or with polybutadiene (PB), an elastomeric material, have been scarcely employed in pervaporative separation.[11,12] However, copolymers of styrene (St) and 1,3-butadiene, namely SBR, have been evaluated as pervaporative membranes for the separation of a few mixtures.[13–15] The employed SBRs usually underwent conventional vulcanization with sulfur to yield crosslinked membranes, and the crosslinking occurred within the butadiene units of the polymeric chains. It is worth pointing out the importance of solvent–polymeric membrane interaction for understanding the separative capacity of the membrane.[16,17]

Of the innumerable binary mixtures whose separations were studied by pervaporation for a matter of purification of one of the components, in Bz/Cx, Bz

Correspondence to: S. Moulay (polymchemlab@hotmail.com or saadmoulay@univ-blida.dz).

is industrially converted to Cx by catalytic hydrogenation, and therefore, its purification by separation is thus required. The intensive research on the pervaporative separation of this system[18–43] witnesses to its peculiarity, which lies mainly on the very close boiling points of the components, 80.103°C for Bz versus 80.738°C for Cx, and on the fact that it is an azeotropic mixture.

We present in this article the use of SBR membranes crosslinked by chloromethylation in the separation of Bz/Cx mixtures. A survey of literature on this issue revealed that such an application of SBR membranes has not been reported yet. Earlier, however, SBR membranes have been employed for the pervaporation separation of Bz/*n*-heptane mixtures.[44,45] Also, the impact of the chloromethylation reaction as a new method of crosslinking SBR on the pervaporation performance is herein reported. In contrast to the vulcanization with sulfur, the crosslinking took places on St units of the polymeric chains via a methylene bridge.

EXPERIMENTAL

Materials

Bz, Cx, chloroform, chlorotrimethylsilane (99% purity), and stannic chloride were purchased from Panreac Quimica (Spain), Merck (Germany), and Fluka (Germany), and were used without further purification. Paraformaldehyde (PF) and SBR containing 45 wt % St were supplied by Aldrich Chemical Co. (France).

Membrane preparation

In a 250-mL, three-necked round-bottom flask fitted with a condenser, a thermometer, and a magnetic bar, we prepared a 2 wt % solution of SBR in chloroform by stirring a quantity of SBR in an appropriate volume of chloroform. To this solution was added a mixture of PF and trimethylchlorosilane (TMCS), and as soon as the PF was dissolved in the system, a volume of 100 μL of stannic chloride was added. The system was then heated at 40°C until gelatinous mass was formed. The time of the gel onset depended on the [St]/[TMCS]/[PF] molar ratio; for molar ratios of 1 : 1 : 1, 1 : 1.5 : 1.5, 1 : 2 : 2, and 1 : 2.5 : 2.5, the times were 15, 8, 4, and 2 min, respectively. As soon as this mass was produced, the mixture was instantaneously poured onto a glass plate and spread evenly over a clean Teflon-plate surface by means of an appropriate applicator. A transparent film was obtained after drying for 24 h at room temperature. The thickness of the membrane (l) was estimated to be 130 ± 1 μm with a micrometer (Micro-Italiana, Italy). Chloromethylation was carried out for the previous [St]/[TMCS]/[PF] molar ratios. Thus, four membranes were evaluated in this study; they were, respectively, SBR_1, $SBR_{1.5}$, SBR_2, and $SBR_{2.5}$.

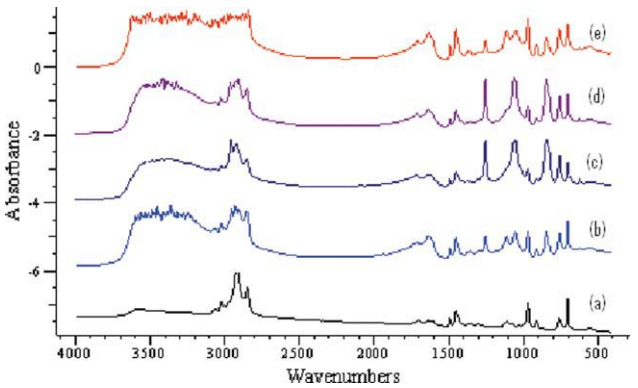

Figure 1 FTIR spectra: (a) noncrosslinked SBR, (b) SBR_1, (c) $SBR_{1.5}$, (d) SBR_2, and (e) $SBR_{2.5}$. [Color figure can be viewed in the online issue, which is available at wileyonlinelibrary.com.]

Membrane characterization

The membranes were characterized by their insolubility and by infrared spectroscopy in the form of thin films (Shimadzu, Japan FTIR-8900; Fig. 1). Scanning electron microscopy (SEM) images of the SBR membranes [Figs. 2(a–e)] were taken at CRNA (Nuclear Research Center of Algiers, Algiers) with an environmental scanning electron microscope (Philips XL30 ESEM–FEG (environmental scanning electron microscope-field emission gun)).

The mechanical properties, tensile strength (σ), and elongation at break (ε_B) of the different membranes were measured (Table I) by an Instron INSTRON 3345 instrument (France), according to the European norm EN 455-2 : 2000.

Estimation of the crosslinking density (v)

v was computed from the Flory–Rehner equation:[46]

$$v = \frac{1}{V_s}\left[\frac{\ln(1-v_r)+v_r+\chi v_r^2}{v_r^{1/3}-\frac{1}{2}v_r}\right] \quad (1)$$

where V_s is the molecular volume of the swelling solvent, v_r is the volume fraction of the polymer measured at the swelling equilibrium state, and χ is the Flory–Huggins interaction parameter. χ and v_r were estimated from eqs. (2) and (3), respectively:

$$\chi = \beta + \frac{V_s}{RT}(\delta_s - \delta_p)^2 \quad (2)$$

$$v_r = \frac{A_d \rho_p^{-1}}{A_d \rho_p^{-1} + A_s \rho_s^{-1}} \quad (3)$$

where β is the entropic factor, taken as 0.34,[47] δ_s is the solubility parameter of the solvent, δ_p is the

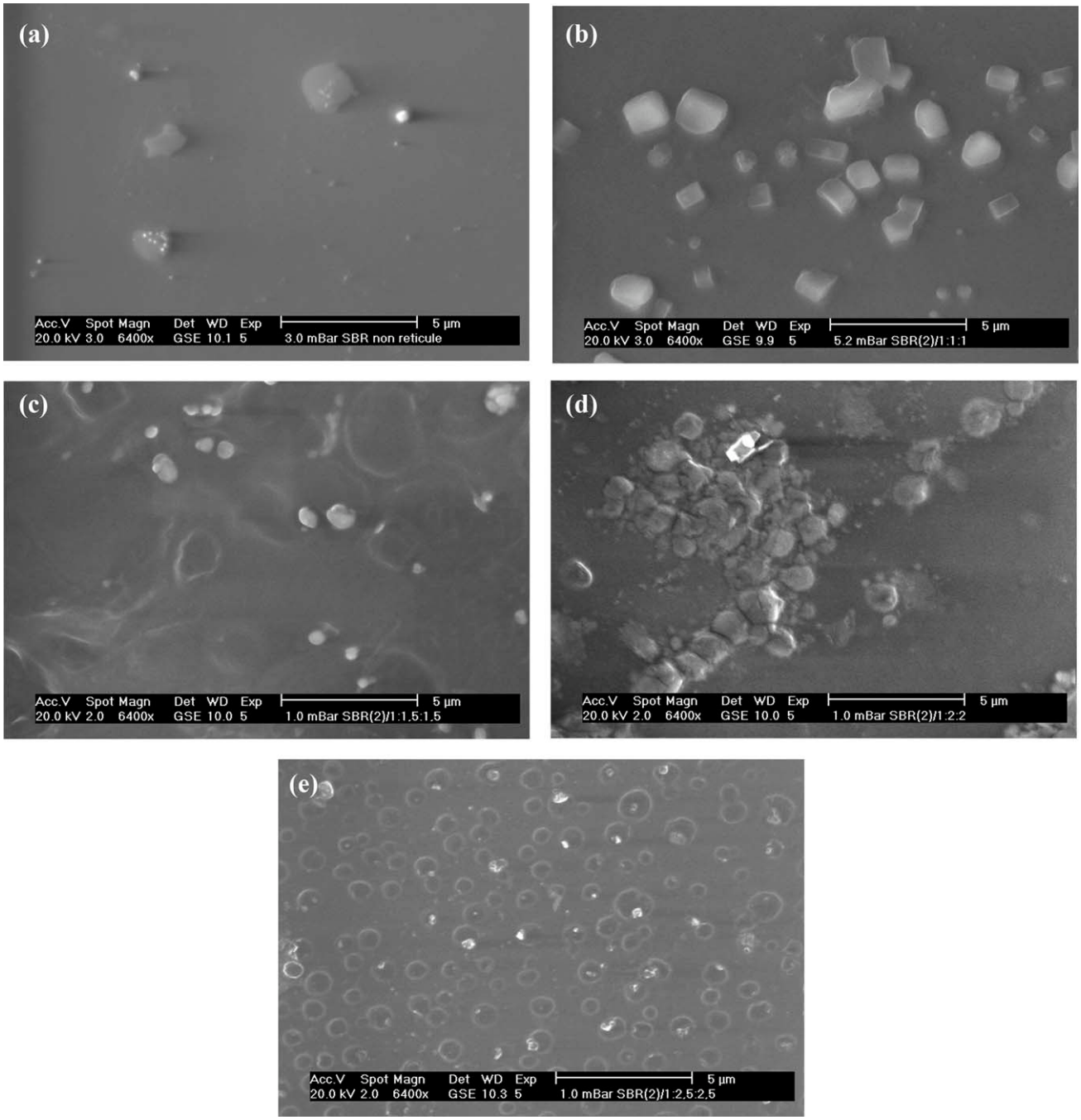

Figure 2 SEM micrographs: (a) noncrosslinked SBR, (b) SBR_1, (c) $SBR_{1.5}$, (d) SBR_2, and (e) $SBR_{2.5}$.

solubility parameter of the polymer, R is the gas constant, T is the temperature (K), A_d is the weight of the dry sample after swelling, rho_p and rho_s are the densities of the polymer and the solvent, respectively and A_s is the weight of the absorbed solvent.

Thermal analyses

Thermogravimetric analysis (TGA) thermograms (Fig. 3) of the different crosslinked SBRs were recorded with a TGA Q50 version 20.2 Build 27 apparatus (England) under an argon atmosphere in the temperature range 0–700°C at a rate of 20°C/min. Differential scanning calorimetry (DSC) thermograms (Fig. 4)

TABLE I
Mechanical Properties of the Membranes

Membrane	ε_B (%)	σ (MPa)
SBR_1	369	2.81
$SBR_{1.5}$	209	4.68
SBR_2	140	6.23
$SBR_{2.5}$	198	6.60

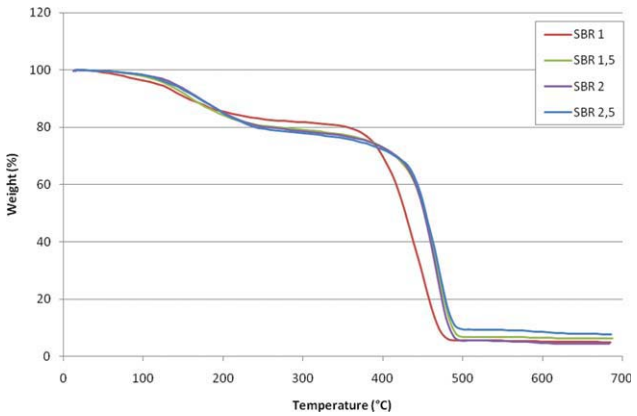

Figure 3 TGA thermograms of the crosslinked SBRs. [Color figure can be viewed in the online issue, which is available at wileyonlinelibrary.com.]

were recorded with a DSC Q100 version 9.8 Build 296 apparatus (England) in the temperature range −80 to 80°C at a rate of 10°C/min.

Membrane sorption

The swelling degrees (S values) of the membranes with Cx and Bz and with 1 : 9 and 1 : 1 v/v Bz/Cx mixtures were determined by eq. (4):

$$S(\%) = \left[\frac{w - w_0}{w_0}\right] \times 100 \tag{4}$$

where w_0 and w are the sample weights before and after swelling, respectively. Before weighing and after the swelling operation, the membrane was rapidly wiped off in a cold area to prevent the loss of the swelling probe.

Sorption selectivity (α_S)

A membrane sample of known weight was immersed into the liquid (Bz, Cx, or mixtures of Bz and Cx), and the whole system was allowed to stand for 48 h at 30°C to reach an equilibrated state. The sample was then drawn out, and the liquid droplets on the surface were rapidly wiped off, as described previously. The sorbed sample was weighed and then placed in one tube of a two-tube device, where the other tube, constituting a cold trap, was immersed into a liquid nitrogen container. The first tube, containing the sorbed membrane, was heated at 30°C *in vacuo* (with a vacuum pump), and the sorbing liquid was collected in the cold trap. The collected liquid was analyzed by gas chromatography under the chromatographic conditions described later. α_S and the diffusion selectivity (α_D) were computed from

$$\alpha_D = \alpha/\alpha_S$$

where α is the separation factor and α_S was estimated by eq. (5)

$$\alpha_S = \frac{M_{Bz}/M_{Cx}}{F_{Bz}/F_{Cx}} \tag{5}$$

where M_{Bz} and M_{Cx} are the weight fractions of benzene and cyclohexane, respectively, in the membrane and F_{Bz} and F_{Cx} are the weight fractions of benzene and cyclohexane, respectively, in the feed.

Pervaporation technique

The pervaporation apparatus used in this study was described previously.[1,2,4–6] It comprised the following parts: a stainless steel pervaporation cell (capacity = 125 cm^3), a pervaporation Pyrex-made receiving set fitted with vapor traps, and primary vacuum pump (160 Pa), Alcatel 2010 (France). The condensation of the pervaporate was done by means of liquid nitrogen.

The liquid permeate was analyzed by gas chromatography with a Shimadzu GC-17A with the following parts: an flame ionization detector (FID) detector, nitrogen as a carrier gas, and a capillary column OV-1701 (25 m in length). The injection-port temperature was 220°C, the column temperature was 40°C, and the detector temperature was 200°C.

The total mass flux rate or permeate flux ($J = J_{Bz} + J_{Cx}$, where J is the total flux) was provided by eq. (6):

$$J(\mathrm{gh^{-1}m^{-2}}) = \frac{W}{tA} \tag{6}$$

where W is the weight of the condensate, t is the trapping time (h), and A is the surface area of the membrane (m^2). The surface area of membrane was

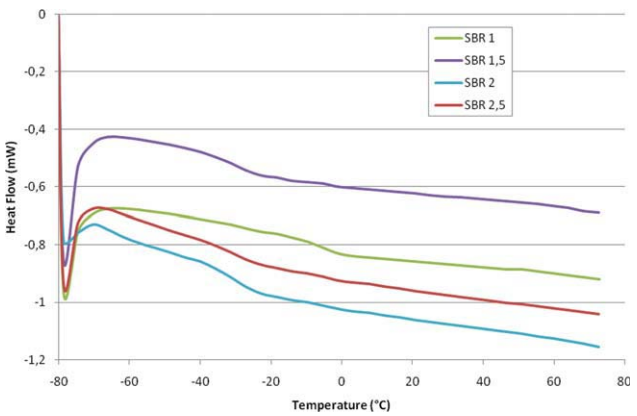

Figure 4 DSC thermograms of the crosslinked SBRs. [Color figure can be viewed in the online issue, which is available at wileyonlinelibrary.com.]

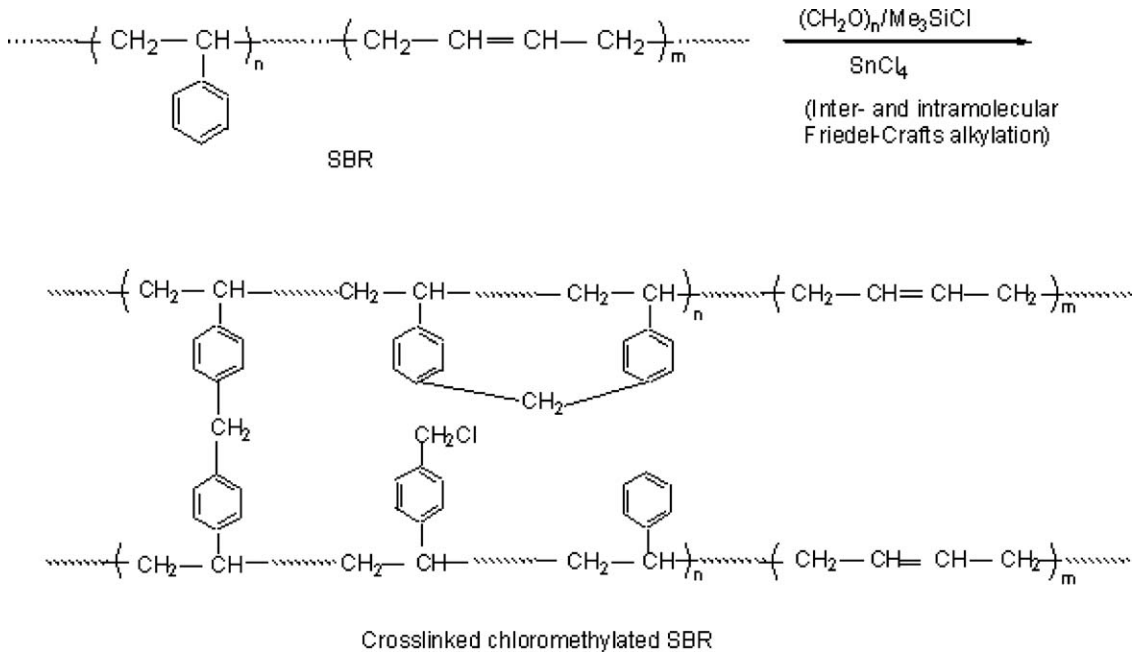

Scheme 1 Chloromethylation of SBR

25.0 cm^2. α was estimated from the following relation:

$$\alpha = (Y_{Bz}/Y_{Cx})/(X_{Bz}/X_{Cx}) \quad (7)$$

where X and Y were the weight fractions of the components in the feed and the permeate, respectively.

Estimation of the diffusion coefficients (*D*s)

The Fickian *D*s of Bz and Cx through the SBR membranes were estimated from the following well-known esquation:[48]

$$\frac{DS_t}{DS_\infty} = 1 - \sum_{n=0}^{\infty} \frac{8}{(2n+1)^2\pi^2} \exp\left[\frac{-D(2n+1)^2\pi^2\tau}{l^2}\right] \quad (8)$$

where τ is time, DS_t and DS_∞ are the equilibrium sorption amounts of Bz (or Cx) per unit mass of the dried membrane (g of Bz or Cx/g of membrane) at time t and infinity, respectively, and l is the thickness of the dried membrane with a weight of m.

At shorter times ($DS_t/DS_\infty \leq 0{,}4$), eq. (4) can be rewritten as in eq. (9):

$$\frac{DS_t}{DS_\infty} = 4\left(\frac{D\tau}{\pi l^2}\right)^{1/2} \quad (9)$$

The latter equation can be rearranged to the following form:

$$D = \frac{\pi}{16}\left(\frac{DS_t/DS_\infty}{\sqrt{\tau}/l}\right) \quad (10)$$

Providing the initial slope (tan θ) of the straight line of the curve $DS_t/DS_\infty = f(\tau^{1/2}/l)$, D can be deduced from the following relation:

$$D = \frac{\pi}{16}(\tan\theta)^2 \quad (11)$$

RESULTS AND DISCUSSION

Preparation and characterization of the SBR membranes

The SBR membrane was subjected to the conditions of chloromethylation described in literature (Scheme 1).[49–51] By now, it is common knowledge to polymer researchers that the chloromethylation of polystyrenics is hampered by the concomitant crosslinking via methylene bridging. The latter, considered a side reaction, can be ensued by *in situ* intermolecular and intramolecular Friedel–Crafts alkylations, and this fact can be monitored by many factors, such as the concentration of the chloromethylating agent, the time, and the temperature.[49,52] It was reported earlier that such a side reaction was advantageous for the realization of soluble poly(3,4-dimethoxy-*o*-tolylene) and poly(2,5-dimethoxy-*p*-tolylene), valuable redox polymer precursors.[53,54]

Instead of being interested in linear chloromethylated polystyrenics, we herein rather exploited this ensuing *in situ* crosslinking for making crosslinked SBR membrane, as illustrated in Scheme 1. Chloromethylation by the $(CH_2O)_{n/}/Me_3SiCl$ system occurred on the phenyl groups of styrenic units,

TABLE II
v Values of the SBR Membranes

	SBR_1	$SBR_{1.5}$	SBR_2	$SBR_{2.5}$
$v \times 10^5$ (Bz)	6.1157	9.1580	21.505	29.197

followed by Friedel–Crafts alkylation; this gave rise to crosslinked SBR. All of the SBRs obtained defied insolubility in common organic solvents, which was evidence of the occurrence of crosslinking; they swelled in chloroform, tetrahydrofuran, dimethyl sulfoxide, Bz, and Cx and were insoluble in methanol and acetone. Figure 1 shows the FTIR spectra of the bare SBR and the cured SBRs. New bands in the spectra of the latter compared to that of the former suggested a successful modification. In Figure 1(a), the bands at 1253 and 844 cm^{-1} were assigned to the residual chloromethyl groups (CH_2Cl),[49] and the band at 1110 cm^{-1} was attributed to the crosslinking methylene group (between the two phenyl groups). It was observed that increases in the TMCS and PF concentrations led to a higher degree of chloromethylation, as evidenced by IR analysis. Thus, the real chemical structure of the crosslinked SBR was a mixture of styrenic units, chloromethylated styrenic units, butadiene units, and 4,4′-disubstitued diphenylmethane units from the crosslinking reaction.

The extent of crosslinking of the different membranes are given in terms of v, which was estimated chemically with Flory–Rehner theory. The values of v are compiled in Table II. v was found to increase with increasing [St]/[TMCS]/[PF] ratio; those values of $SBR_{2.5}$ and SBR_2 were nearly five-fold and three-and-a-half-fold that of SBR_1. Such curing raised the glass-transition temperature stemming from the restrictions of the polymeric matrices. Indeed, as seen in Figure 4, the glass-transition temperatures of the cured SBRs were in the range of −30°C, with values higher than that of pristine SBR (−55°C).

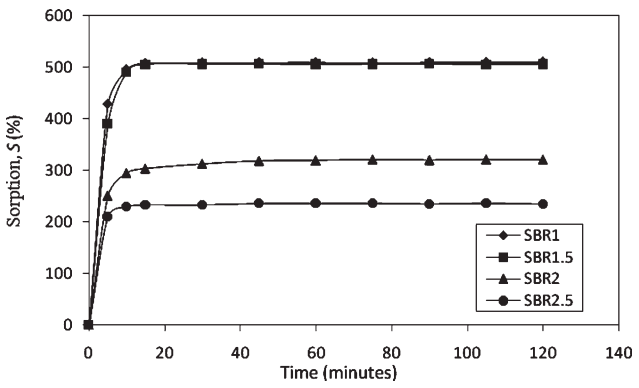

Figure 5 Plots of the variations of swelling of the different membranes by Bz at 30°C as a function of time.

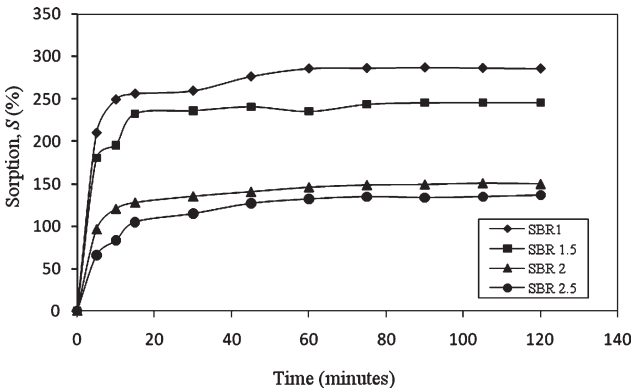

Figure 6 Plots of the variations of swelling of the different membranes by Cx at 30°C as a function of time.

TGA thermograms (Fig. 3) revealed the thermal stability of the cured SBRs up to 400°C. Yet, a degradation starting at 90°C and finishing at 200°C were noticed and were probably due to dechloromethylation of the residual chloromethyl groups.

Figures 2(a–e) exhibit the surface morphologies of pristine and crosslinked SBR membranes upon their examination with SEM. A difference in the surface morphology was noticed between the noncrosslinked and crosslinked SBR membranes. Although that of bare SBR was almost plain, even, continuous and smooth, those of the crosslinked SBRs were rough, coarse, and in some cases, discontinuous; generally, the higher the [St]/[TMCS]/[PF] molar ratio was, the coarser the morphology was. Interesting was the surface morphology of the $SBR_{2.5}$; a distinct uniform globular pattern was created.

The membranes were also characterized by their mechanical strengths. As compiled in Table I, σ rose and ε_B generally dropped with increasing [St]/[TMCS]/[PF] ratio. A higher crosslinking would induce a stiffer material, requiring larger stress to break and a reduction of its elastomeric properties.

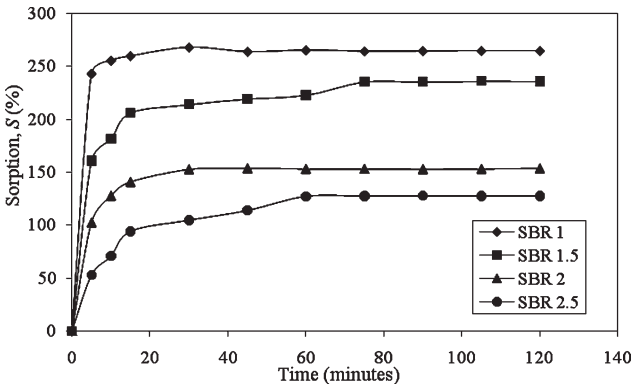

Figure 7 Plots of the variations of swelling of the different membranes by the 1 : 9 Bz/Cx mixture at 30°C as a function of time.

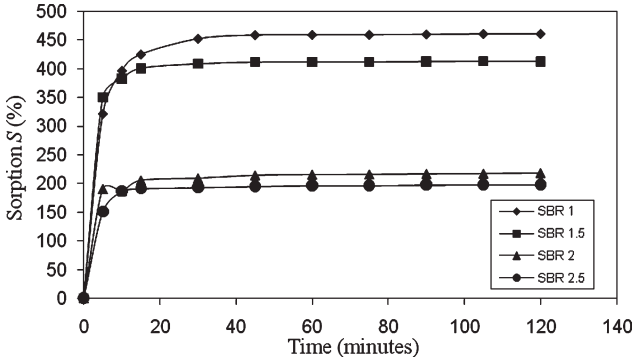

Figure 8 Plots of the variations of swelling of the different membranes by the 1 : 1 Bz/Cx mixture at 30°C as a function of time.

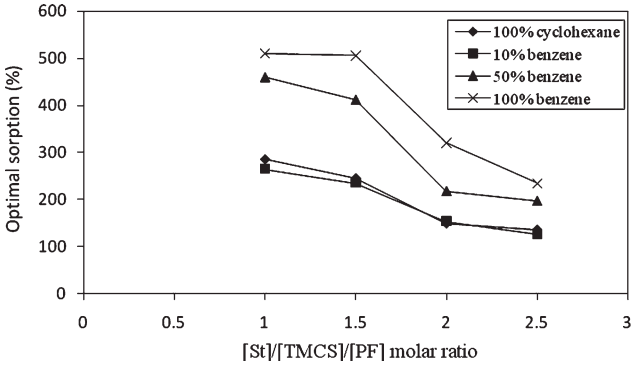

Figure 9 Maximum sorption of the different systems as a function of the [St]/[TMCS]/[PF] molar ratio.

Sorption and diffusion study

Sorption

The swelling capacities of the different SBR membranes were tested in Bz, Cx, and 1 : 1 and 1 : 9 v/v Bz/Cx mixtures as a function of time (Figs. 5–9) at 30°C. It could be seen that the maximum sorption for all systems was completed in relatively shorter times, nearly less than 30 min, and was in the range 280–500%. This may have stemmed from the great chemical affinities of the components toward St and butadiene units of SBR, being all hydrocarbons. The swelling capacity (Fig. 9) decreased with increasing [St]/[TMCS]/[PF] molar ratio; the higher the ratio was, the tighter the crosslinking was and the tougher the SBR membrane was. This fact thus lowered the swelling process. Overall, the SBR membranes showed greater swelling in Bz and Bz-containing mixtures than in Cx. Also, as expected, the lesser the crosslinking was (SBR_1 with a v of 6.116, as shown in Table II), the higher the sorption was. The sorption results were in a good agreement with the theory of Hansen solubility parameters (δ_{HSP}'s); indeed, the rule stating that the smaller the $\Delta\delta_{ij}$ is, the greater the affinity between two substances i and j are, was well verified. According to Table III, the $\Delta\delta$ values for Bz with SBR, PB, and PS were 0.48, 0.52, and 4, respectively, against 1.82, 1.78, and 6.3 for Cx. Both units of SBR comprised unsaturations (π bonds), which made them more vulnerable to the interaction with Bz molecules (with six π electrons) than Cx, a saturated molecule. Therefore, in every respect, the sorption of Bz by SBR was expected to be greater than that of Cx.

D values

The different curves of $DS_t/DS_\infty = f(\tau^{1/2}/L)$ for Bz and Cx and for the four membranes in study are shown in Figure 10. The results of the D values of Bz and Cx at 30°C are compiled in Table IV. As shown, the D values of Bz through the SBR membranes were generally higher than those for Cx. These results further endorse the observation of the larger sorption of Bz by SBR membranes compared with that of Cx. α_D (diffusion coefficient of Bz (D_{Bz})/diffusion coefficient of Cx (D_{Cx})) was in the range of 1.54, 1.67, and 1.53 for SBR_1, $SBR_{1.5}$, and SBR_2, respectively. More conspicuously was the α_D (D_{Bz}/D_{Cx}) for $SBR_{2.5}$, that is, D of Bz in the case of this membrane was nearly three-fold that of Cx. The latter finding suggested that the tighter the crosslinking was, the higher α_D was.

Pervaporation study

Effect of crosslinking

J and α were measured at 30°C as a function of the extent of crosslinking of the membrane or the [St]/[TMCS]/[PF] molar ratio for systems 1 : 1 and 1 : 9

TABLE III
Some Parameters of Bz, Cx, PS, PB, and SBR

	Diffusional cross section (Å^2)[42]	Molar volume (cm^3/mol)[55]	Collision diameter (nm)[55]	δ_{HSP} (MPa$^{1/2}$)
Bz	24.80	89.40	0.526	18.50[56]
Cx	31.30	108.70	0.606	16.20[56]
PS	—	—	—	22.50[56]
PB	—	—	—	17.98[56]
SBR	—	—	—	18.02[57]

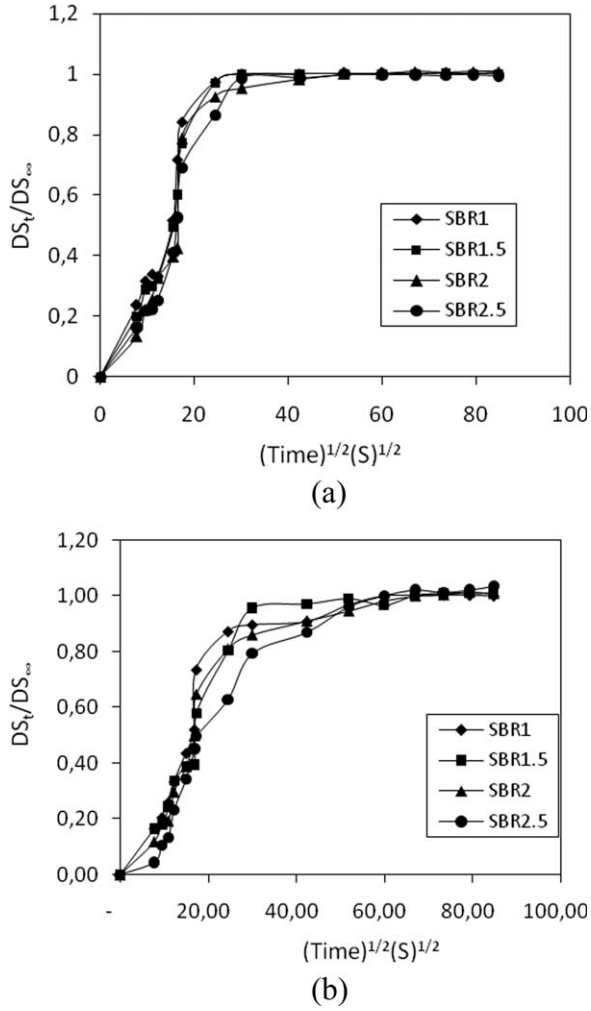

Figure 10 Plots of the variation of DS_t/DS_∞ as a function of $\tau^{1/2}/l$ of the different membranes in (a) Bz and (b) Cx (temperature = 30°C).

(Figs. 11 and 12). In Figure 11, it can be noticed that as the molar ratio increased, the flux for the 1 : 1 and 1 : 9 mixtures decreased. However, that of the first mixture was generally higher than that of the second one. This finding was in accord with the fact that the tighter the network was, the more onerous the permeation experienced by the components was. A relatively facile transport of Bz through the membrane due to its greater sorption as discussed above occurred, as shown in Figure 11. Also, with a Bz-rich mixture (1 : 1), the polymeric network would

TABLE IV
***D*s of Bz and Cx at 30°C**

Membrane	$D_{Bz} \times 10^8$ (m^2/s)	$D_{Cx} \times 10^8$ (m^2/s)
SBR_1	2.45	1.59
$SBR_{1.5}$	1.86	1.12
SBR_2	1.23	0.80
$SBR_{2.5}$	1.02	0.31

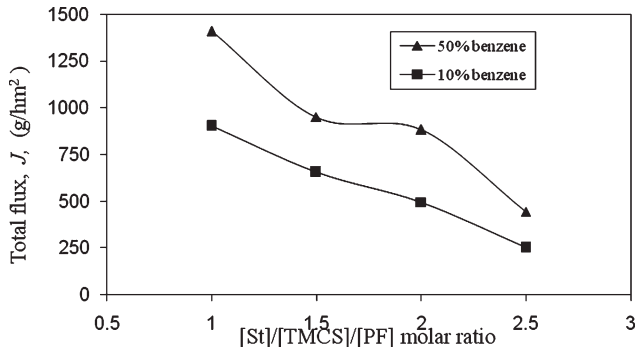

Figure 11 Plot of the variation of *J* as a function of the [St]/[TMCS]/[PF] molar ratio (temperature = 30°C, time = 1 h).

have expanded substantially because the membrane swelled distinctly in Bz, thus allowing a more appreciable transport. Raising the TMCS and PF by two-and-a-half-fold provoked a decline of *J* by three-fold, from nearly 1400 g m^{-2} h^{-1} to about 500 g m^{-2} h^{-1}. As shown in Table V and other reported results,[31–35] the magnitudes of *J* were among the good ones. α, or selectivity, for the 1 : 1 mixture was relatively low for membranes SBR_1 and $SBR_{1.5}$ but slightly increased for SBR_2 and $SBR_{2.5}$, not exceeding a value of 13. With a 1 : 9 mixture, the profile of the variation of α with the extent of crosslinking was clearly different; whereas its values were about 2.5–4 for the first membranes; they were conspicuously higher for the latter two membranes. Indeed, values as high as 17.5 and 28.5 were calculated. Again, the more dense the membrane was, the more selective its behavior was vis-à-vis the binary system. Bz was separated preferentially because of its affinity to the membrane ($\Delta\delta = 0.48$) coupled with its higher sieving capacity; that is, its diffusional cross section, molar volume, and collision diameter were smaller than those of Cx (Table III).

The pervaporation separation index (PSI = $J \times \alpha$) gives an insight into the performance of the membrane in pervaporative separation; the greater PSI is,

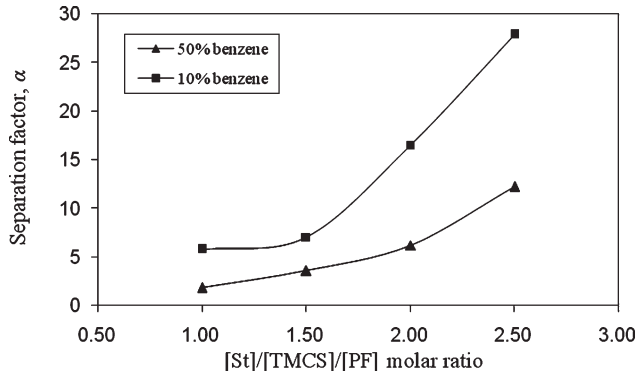

Figure 12 Plot of the variation of α as a function of the [St]/[TMCS]/[PF] molar ratio (temperature = 30°C, time = 1 h).

TABLE V
Comparative Results of the Pervaporative Parameters, *J*, and α, of the Separation of the Bz/Cx Mixtures with Different Membranes (See the References)

Membrane	Bz in feed (wt %)	Temperature (°C)	J (g m^{-2} h^{-1})	α	Reference
SBR_1	10	30	901	5.78	This study
SBR_1	50	30	1401	1.83	This study
P(AN-*b*-MA)	50	30	4200[a]	10.50	18
Pebax (2533)	10	30	800	2.50	19
Pebax (2533)	50	30	4250	1.80	19
PVC	50	30	60.30	9.80	20
PVC–B-10	50	30	40.40	9.43	20
PVC–RhB-10	50	30	56.00	17.38	20
PVA	50	50	21.87	16.70	22
PVA–CMS-06	50	50	59.25	23.21	22
PVA	50	50	22.40	9.60	23
CG–PVA/CS (1 : 1)	50	50	51.40	49.90	23
PU	54	25	263,600[a]	2.50	24
PVA–CG	10	50	40.20	344.50	25
PVA–CG	50	50	90.20	100.10	25
PMMA–Polyelect	20	50	3700	4.10	26
CA	50	70	10	65	27
CA–DNP	50	70	10	103	27
Na(I)–Neosepta	50	25	281	1.15	28
Cu(II)–Neosepta	50	25	841	3.42	28
PVC–EVA	10	30	65	15	30
PVC–EVA	50	30	158	3.2	31

PVC, poly(vinyl chloride); P(AN-*b*-MA), polyacrylonitrile-*block*-poly(methyl acrylate); Pebax (2533), poly(ether-*block*-amide); PVC–B-10, PVC filled with H-β-zeolite in a mass ratio of 0.10; PVC–RhB-10, PVC filled with Rh/H-β-zeolite in a mass ratio of 0.10; PVA, poly(vinyl alcohol); PVA–CMS-06, poly(vinyl alcohol) filled with carbon molecular sieve in a mass ratio of 0.06; CG–PVA/CS (1 : 1), blend of poly(vinyl alcohol) and chitosan filled with carbon graphite-filled; PU, polyurethane; PVA–CG, poly(vinyl alcohol) filled with crystalline flake graphite; PMMA–Polyelect, 1 wt % poly[methyl methacrylate-*co*- methacrylic acid(3-sulfopropyl ester) potassium salt] 7.5 : 1 and 10 wt % benzyldodecyldimethylammonium chloride; CA, cellulose acetate; CA–DNP, cellulose acetate with a dinitrophenyl group as a selective fixed carrier; Na(I)–Neosepta, Cu(II)–Neosepta, cation-exchange membrane in Na(I) and Cu(II) forms, respectively, containing 45–65% sulfonated St/divinylbenzene random copolymer and 45–55% PVC; PVC–EVA, a blend of PVC and low-molecular-weight ethylene-*co*-vinyl acetate copolymer with 38 wt % VA content.
[a] Normalized flux (kg μm m^{-2} h^{-1}).

the more performing the membrane will be. According to the magnitudes of PSI shown in Table VI, the SBR membrane well suited for a good separation of the Bz/Cx mixture was SBR_2. In fact, the highest values of PSI were 5475.74 and 8184.27 for the 1 : 1 and 1 : 9 mixtures, respectively; that is, the lower the Bz content was, the better α was. Overall, the first mixture was more favorable for a good separation employing an SBR membrane.

Effect of the composition feed

The variations of the permselectivity parameters as a function of the feed composition for the different

TABLE VI
SBR Membrane Performance for the Separation of the Bz/Cx Mixture

	1 : 1 Bz/Cx mixture			1 : 9 Bz/Cx mixture		
Membrane	J (g m^{-2} h^{-1})	α	PSI[as]	J (g/m^2 h)	α	PSI
SBR_1	1401.27	1.83	2567.12	901.13	5.78	5214.84
$SBR_{1.5}$	950.23	3.58	3398.02	654.73	7.07	4627.60
SBR_2	883.25	6.20	5475.74	494.90	16.54	8184.27
$SBR_{2.5}$	443.64	12.26	5441.64	249.98	27.89	6972.67

Feed temperature = 30°C; l = 130 μm.
[a] PSI = α × J.

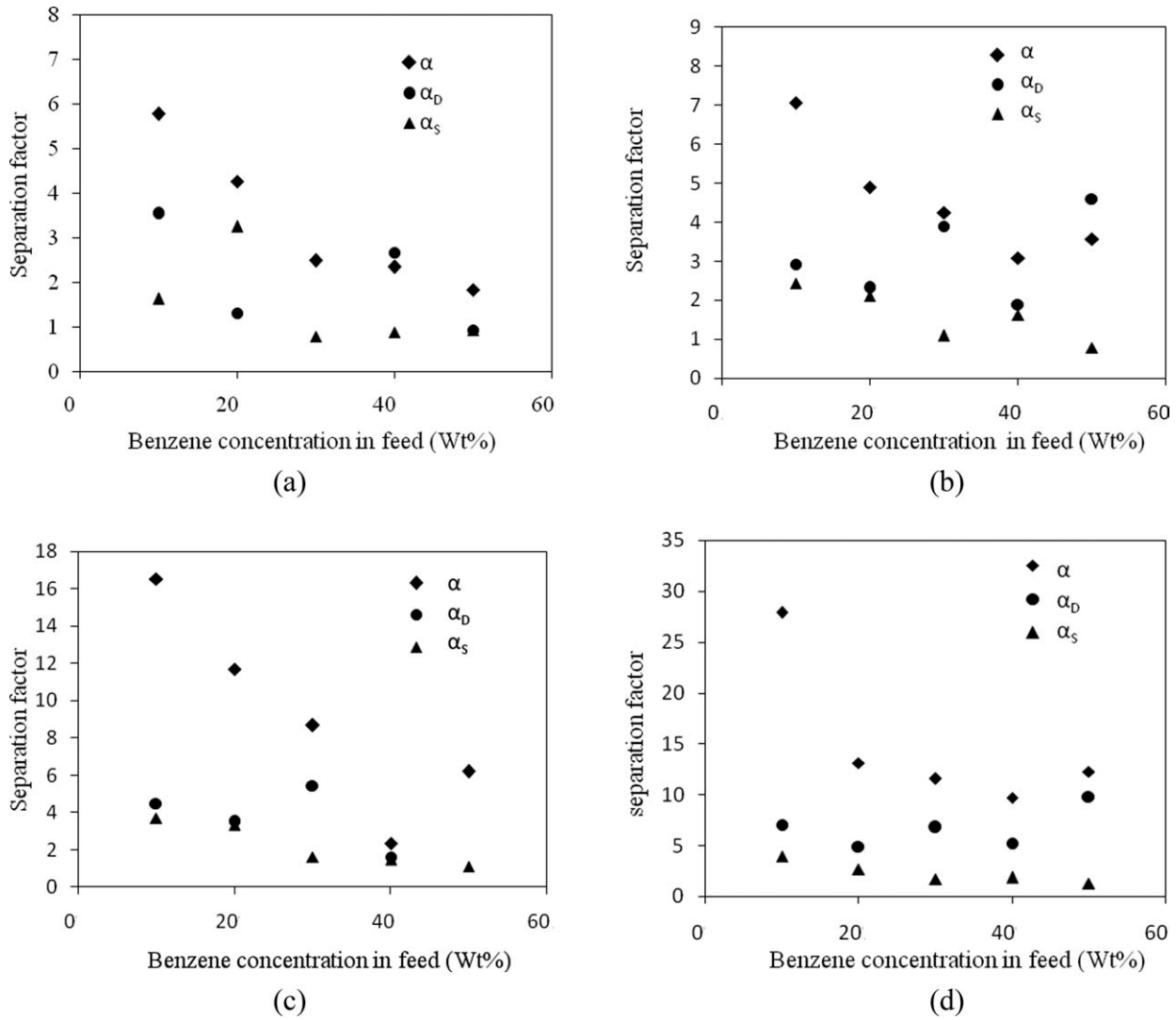

Figure 13 Plots of the variations of the pervaporation selectivity (α, α_D, and α_S) as a function of the Bz concentration in the feed: (a) SBR_1, (b) $SBR_{1.5}$, (c) SBR_2, and (d) $SBR_{2.5}$.

SBR membranes are illustrated in Figures 13(a–d), 14, and 15. The results were that, as often observed, an increase in the Bz content of the feed led to an increase in the permeation flux at the cost of α. This fact was attributed to the membrane plasticization, which resulted in good swelling at higher Bz levels

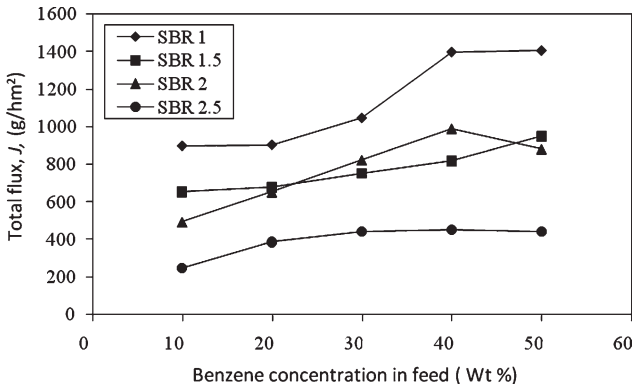

Figure 14 Plots of the variations of J as a function of the Bz concentration in the feed (temperature = 30°C, time = 1 h).

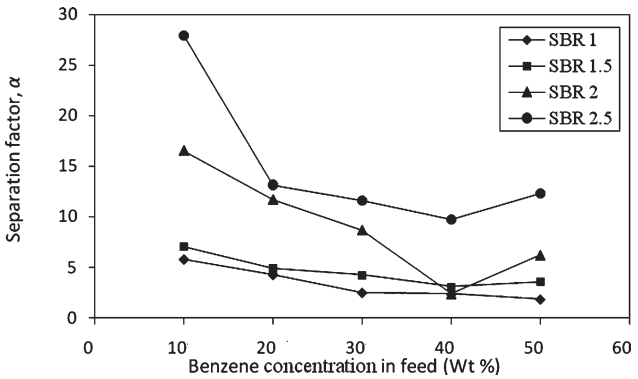

Figure 15 Plots of the variations of α as a function of the Bz concentration in the feed (temperature = 30°C, time = 1 h).

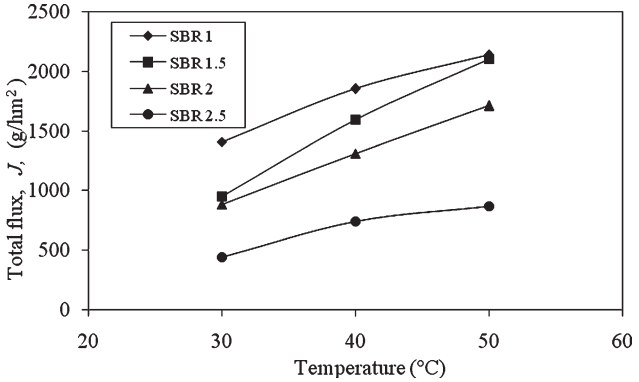

Figure 16 Plots of the variations of J as a function of the temperature for the 1 : 1 system.

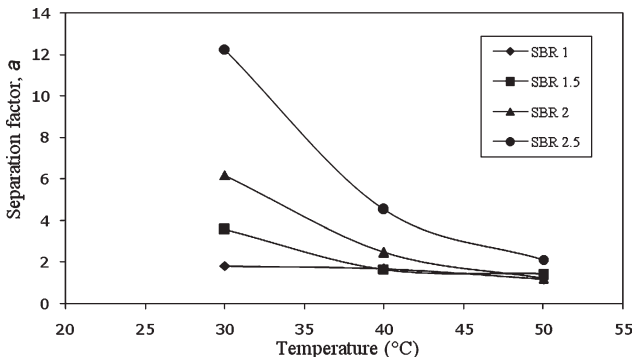

Figure 17 Plots of the variation of α as a function of the temperature for the 1 : 1 system.

in the feed. On the basis of the geometrical considerations and solubility parameters (Table III), Bz was expected to permeate more preferentially, but the actual results (ours and others') suggested that good swelling of the membrane would have permitted the transport of both components with closer rates.

In Figures 13(a–d), the different selectivities (α, α_D, and α_S) are plotted against the Bz content in the feed for each membrane. It can be noticed their variations did not follow systematic patterns, but the general trend was $\alpha > \alpha_D > \alpha_S$; this indicated that the diffusion at the bottom layer of the membrane was mainly responsible for the pervaporation course. It is known that α_D is tightly bound to, besides the size of the diffusing probe, the internal architecture of the membrane; that is, the denser the membrane is, the higher α_D will be. It can be also noted that all of sthe selectivities nearly decreased with increasing Bz in the feed; this suggested the component size factor did not prevail, as stated previously.

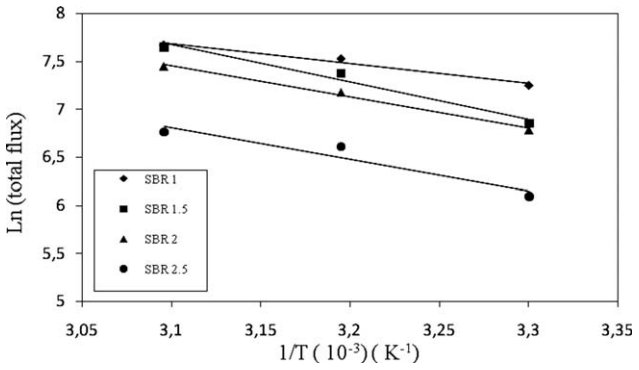

Figure 18 Arrhenius plot of J [Ln $J = f(1/T)$] for the 1 : 1 system.

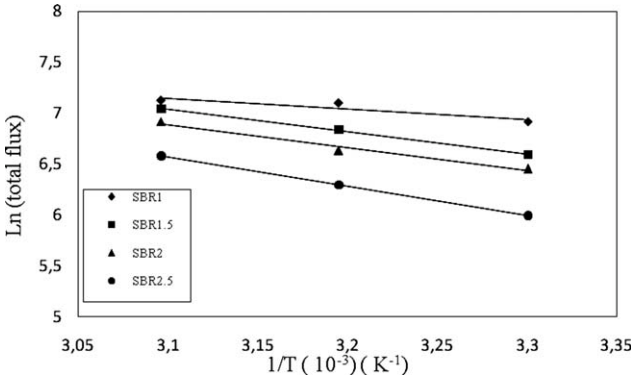

Figure 19 Arrhenius plot of J [Ln $J = f(1/T)$] for Bz.

Effect of temperature

In the case of the Bz/Cx 1 : 1, the influence of temperature on both J and α was obvious. As shown in Figures 16 and 17, with increasing working temperature, J increased and α generally decreased. It seemed that the selectivity reached its lowest value at 50°C and remained constant beyond this temperature. However, the flux continued to augment, particularly for SBR_2.

In Figures 18–20, the Arrhenius relation, Ln $J = f(1/T)$, is plotted for different SBR membranes and for Cx, Bz, and a 1 : 1 Bz/Cx mixture. As gathered in Table VII, the corresponding activation energies (E_a's) were estimated to be nearly 2–6, 7–15, and 4–8 Kcal/mol, respectively. It is clear that SBR_1 favored

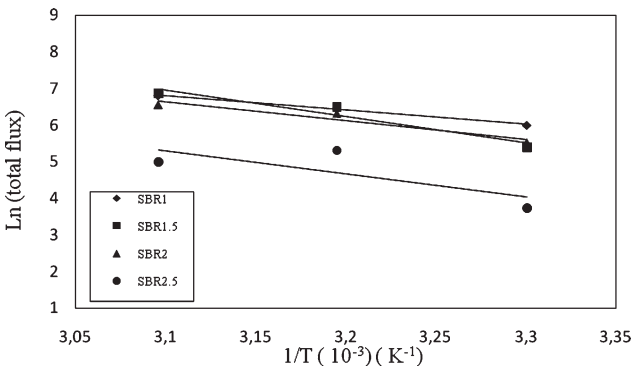

Figure 20 Arrhenius plot of J [Ln $J = f(1/T)$] for Cx.

TABLE VII
E_a's of the Permeation of Bz, Cx, and a 1 : 1 Bz/Cx Mixture through the SBR Membranes

	E_a (kcal mol^{-1} K^{-1})		
	Bz	Cx	1 : 1 Bz/Cx mixture
SBR_1	2.066	7.906	4.40
$SBR_{1.5}$	4.406	14.496	7.75
SBR_2	4.548	10.186	6.45
$SBR_{2.5}$	5.718	12.496	6.56

the highest J, as suggested by its lowest E_a, and the trend in the permeation capacity was generally in line with the value of this energy. Also, it can be remarked that E_a seemed to level off for [St]/[TMCS]/[PF] ratios higher than 1 : 2.5 : 2.5; that is, it became independent at higher crosslinking extents. In other words, the pervaporative factors remained unchanged beyond a certain crosslinking extent, a fact that was observed earlier.[1,58] Again, the higher permeation of Bz compared with Cx was supported by the lower E_a. It is interesting to notice that E_a for the 1 : 1 Bz/Cx mixture was within the mean range.

CONCLUSIONS

Membranes made from a chloromethylation-promoted crosslinking of SBR were efficient in the pervaporative separation of Bz–Cx mixtures. SBR membranes crosslinked with a [St]/[TMCS]/[PF] ratio of 1 : 2 : 2 were more suited for good permselectivity performance. The sizes of the permeating species, Bz and Cx, had a little effect on the preferential transport.

The authors thank Nassim Souami (CRNA, Algiers) and Mrs. Fatima-Zohra Mouhabeddine (Laboratoire Nationale de Contrôle des Produits Pharmaceutiques, Chéraga, Algiers) for their kind help in performing SEM analyses and mechanical strength testing, respectively.

References

1. Benguergoura, H.; Aouak, T.; Moulay, S. J Membr Sci 2004, 229, 107.
2. Wynn, N. Chem Eng Prog 2001, 97, 66.
3. Delgado, P.; Sanz, M. T.; Beltrán, S. J Membr Sci 2009, 332, 113.
4. Aminabhavi, T. M.; Aithal, U. S.; Shukla, S. S. J Macromol Sci Rev Macromol Chem Phys 1989, 29, 319.
5. Aminabhavi, T. M.; Khinnavar, R. S.; Harogoppad, S. B.; Aithal, U. S.; Nguyen, Q. T.; Hansen, K. C. J Macromol Sci Rev Macromol Chem Phys 1994, 34, 139.
6. Moulay, S.; Hadj-Ziane, A.; Canselier, J. P. J Colloid Interface Sci 2007, 311, 556.
7. Moulay, S.; Hadj-Ziane, A.; Bensacia, N. Sep Purif Technol 2005, 44, 181.
8. Aouak, T.; Moulay, S.; Hadj-Ziane, A. J Membr Sci 2000, 2, 149.
9. Aminabhavi, T. M.; Kulkarni, P. V.; Kurkuri, M. U.S. Pat. 7,045,062 B1 (2006).
10. Buckley-Smith, M. K. Ph.D. dissertation, University of Waikato, 2006.
11. Shao, P.; Huang, R. Y. M. J Membr Sci 2007, 287, 162.
12. Smitha, B.; Suhanya, D.; Sridhar, S.; Ramakrishna, M. J Membr Sci 2004, 241, 1.
13. Ray, S.; Ray, S. K. J Membr Sci 2006, 270, 132.
14. Jitesh, K. D.; Pangarkar, V. G.; Niranjan, K. Bioseparation 2000, 9, 145.
15. George, S. C.; Prasad, K.; Misra, J. P.; Thomas, S. J Appl Polym Sci 1999, 74, 3059.
16. Aminabhavi, T. M.; Harogoppad, S. B.; Khinnavar, R. S.; Balundgi, R. H. J Macromol Sci Rev Macromol Chem Phys 1991, 31, 433.
17. Ortego, J. D.; Aminabhavi, T. M.; Harlapur, S. F.; Balundgi, R. H. J Hazard Mater 1995, 42, 115.
18. An, Q. F.; Qian, J. W.; Zhao, Q.; Gao, C. J. J Membr Sci 2008, 313, 60.
19. Yildirim, A. E.; Hilmioglu, N. D.; Tulbentci, S. Desalination 2008, 219, 14.
20. Zhang, X.; Qian, L.; Wang, H.; Zhong, W.; Du, Q. Sep Purif Technol 2008, 63, 434.
21. Bai, Y. X.; Qian, J. W.; Zhao, Q.; Xu, Y.; Ye, S. R. J Appl Polym Sci 2006, 102, 2832.
22. Sun, H. L.; Lu, L. Y.; Peng, F. B.; Jiang, Z. Y. Sep Purif Technol 2006, 52, 203.
23. Lu, L. Y.; Sun, H. L.; Peng, F. B.; Jiang, Z. Y. J Membr Sci 2006, 281, 245.
24. Wolinska-Grabczyk, A. J Membr Sci 2006, 282, 225.
25. Peng, F. B.; Lu, L. Y.; Hu, C. L.; Wu, H.; Jiang, Z. Y. J Membr Sci 2005, 259, 65.
26. Schwarz, H. H.; Malsch, G. J Membr Sci 2005, 247, 143.
27. Kusumocahyo, S. P.; Ichikawa, T.; Shinbo, T.; Iwatsubo, T.; Kameda, M.; Ohi, K.; Yoshimi, Y.; Kanamori, T. J Membr Sci 2005, 253, 43.
28. Lue, S. J.; Wang, F. J.; Hsiaw, S. Y. J Membr Sci 2004, 240, 149.
29. Pandey, L. K.; Saxena, C.; Dubey, V. J Membr Sci 2003, 227, 173.
30. An, Q. F.; Qian, J. W.; Sun, H. B.; Wang, L. N.; Zhang, L.; Chen, H. L. J Membr Sci 2003, 222, 113.
31. Kao, S. T.; Wang, F. J.; Lue, S. J. Desalination 2002, 149, 35.
32. Yildirim, A. E.; Hilmioglu, N. D.; Tulbentci, S. Chem Eng Technol 2001, 24, 275.
33. Villaluenga, J. P. G.; Tabe-Mohammadi, A. J Membr Sci 2000, 169, 159.
34. Yoshikawa, M.; Tsubouchi, K. Sep Sci Technol 2000, 35, 1863.
35. Yoshikawa, M.; Shimada, H.; Tsubouchi, K.; Kondo, Y. J Membr Sci 2000, 177, 49.
36. Yoshikawa, M.; Tsubouchi, K. Sep Purif Technol 1999, 17, 213.
37. Yoshikawa, M.; Tsubouchi, K. J Membr Sci 1999, 158, 269.
38. Kusakabe, K.; Yoneshige, S.; Morooka, S. J Membr Sci 1998, 149, 29.
39. Inui, K.; Tsukamoto, K.; Miyata, T.; Uragami, T. J Membr Sci 1998, 138, 67.
40. Yoshikawa, M.; Kitao, T. Eur Polym J 1997, 33, 25.
41. Yoshikawa, M.; Takeuchi, S.; Kitao, T. Angew Makromol Chem 1997, 245, 193.
42. Ray, S. K.; Sawant, S. B.; Joshi, J. B.; Pangarkar, V. G. Ind Eng Chem Res 1997, 36, 5265.
43. Inui, K.; Okumura, H.; Miyata, T.; Uragami, T. J Membr Sci 1997, 132, 193.
44. Brun, J. P. U.S. Pat. 3,930,990 (1976).
45. Brun, J. P.; Larchet, C.; Guillou, M. J Membr Sci 1983, 15, 81.
46. Boonstra, B. B. In Rubber Technology and Manufacture, 2nd ed.; Blow, C. M., Hepburn, C., Eds.; Butterworth Scientific: London, 1982; p 269.
47. Marzocca, A. J. Eur Polym J 2007, 43, 2682.

48. Chen, H. L.; Wu, L. G.; Tan, J.; Zhu, C. I. Chem Eng J 2000, 78, 159, and references therein.
49. Moulay, S.; Nadia, N. Chin J Polym Sci 2006, 24, 627.
50. Avram, E. Polym Plast Technol Eng 2001, 40, 275.
51. Avram, E.; Butuc, E.; Luca, C.; Druta, I. J Macromol Sci Pure Appl Chem A 1997, 34, 1701.
52. Bicak, N.; Koza, G.; Yagci, Y. J Polym Mater 1992, 8, 189.
53. Moulay, S.; M'zyène, F. Chin J Polym Sci 2006, 24, 41.
54. Moulay, S.; M'zyène, F. J Alger Chem Soc 2006, 16, 109.
55. Stichlmair, J. G.; Fair, J. R. Distillation: Principles and Practices; Wiley: New York, 1998.
56. Hansen, C. M. Hansen Solubility Parameters: A User's Handbook, 2nd ed.; CRC and Taylor & Francis: New York, 2007.
57. Utracki, L. A. Polymer Blends Handbook; Kluwer Academic: Dordrecht, The Netherlands, 2003.
58. Bennett, M.; Brisdon, B. J.; England, R.; Field, R. W. J Membr Sci 1997, 137, 63.